Published in final edited form as:
Cell Metab. 2012 May 2; 15(5): 752–763. doi:10.1016/j.cmet.2012.03.020.

Ablation of Steroid Receptor Coactivator-3 resembles the human CACT metabolic myopathy

Brian York[1,¶], **Erin L. Reineke**[1,¶], **Jørn V. Sagen**[2,3], **Bryan C. Nikolai**[1], **Suoling Zhou**[1], **Jean-Francois Louet**[1], **Atul R. Chopra**[1], **Xian Chen**[1], **Graham Reed**[4], **Jeffrey Noebels**[4], **Adekunle M. Adesina**[5], **Hui Yu**[6], **Lee-Jun C. Wong**[6], **Anna Tsimelzon**[7], **Susan Hilsenbeck**[7], **Robert D. Stevens**[8], **Brett R. Wenner**[8], **Olga Ilkayeva**[8], **Jianming Xu**[1], **Christopher B. Newgard**[8,¶], and **Bert W. O'Malley**[1,††,¶]

[1]Department of Molecular and Cellular Biology, Baylor College of Medicine, Houston, TX 77030

[2]Institute of Medicine, University of Bergen, Bergen, Norway N-5021

[3]The Hormone Laboratory, Haukeland University Hospital, Bergen, Norway N-5021

[4]Department of Neurology, Baylor College of Medicine, Houston, TX 77030

[5]Department of Pathology, Texas Children's Hospital, Houston, TX 77030

[6]Department of Molecular and Human Genetics, Baylor College of Medicine, Houston, TX 77030

[7]Lester and Sue Smith Breast Center, Baylor College of Medicine, Houston, TX 77030

[8]Sarah W. Stedman Nutrition and Metabolism Center, Duke University Medical School, Durham, NC 27704

Summary

Oxidation of lipid substrates is essential for survival in fasting and other catabolic conditions, sparing glucose for the brain and other glucose-dependent tissues. Here we show Steroid Receptor Coactivator-3 (SRC-3) plays a central role in long chain fatty acid metabolism by directly regulating carnitine/acyl-carnitine translocase (*CACT*) gene expression. Genetic deficiency of *CACT* in humans is accompanied by a constellation of metabolic and toxicity phenotypes including hypoketonemia, hypoglycemia, hyperammonemia, and impaired neurologic, cardiac and skeletal muscle performance, each of which is apparent in mice lacking SRC-3 expression. Consistent with human cases of CACT deficiency, dietary rescue with short chain fatty acids drastically attenuates the clinical hallmarks of the disease in mice devoid of SRC-3. Collectively, our results position SRC-3 as a key regulator of β-oxidation. Moreover, these findings allow us to consider platform coactivators such as the SRCs as potential contributors to syndromes such as CACT deficiency, previously considered as monogenic.

[††]Corresponding Author: Bert W. O'Malley, M.D., Department of Molecular and Cellular Biology, Baylor College of Medicine, 1 Baylor Plaza, Houston, TX 77030, Phone: 713-798-6205, berto@bcm.edu.
[¶]These authors contributed equally to this work.

Introduction

During fasting or prolonged exercise, mitochondrial fatty acid metabolism is activated in skeletal muscle to protect glucose-dependent tissues such as the brain. This metabolic switch in skeletal muscle is controlled by tightly coordinated transcriptional and allosteric regulatory events that prime the mitochondrial β-oxidation machinery for utilization of lipid substrates. During periods of exertion when energy demand exceeds the mitochondrial capacity to deliver ATP, the muscle reverts to a less efficient anaerobic pathway, eventually depleting the body of glucose and forcing the cessation of exercise.

The mitochondrial β-oxidation system encompasses a set of at least 25 enzymes and transport proteins to facilitate highly efficient harvesting of energy from fatty acids (Eaton et al., 1996). To date, deficiencies in 22 of these proteins have been directly linked to a variety of human metabolic diseases (Moczulski et al., 2009). While there are several points of regulation for fatty acid metabolism, a critical step is the transport of fatty acids into the mitochondria. This process is governed by the carnitine transport system, where the enzymes carnitine palmitoyltransferase I and II (CPTI and CPTII) are functionally linked to the activity of CACT, making this translocase a central regulator of fatty acid metabolism (McGarry and Brown, 1997). Akin to other defects in β-oxidation, deficits in *CACT* gene expression or activity present as a constellation of clinical symptoms arising from energy depletion and toxicity of accumulating lipid species and other metabolites (Roschinger et al., 2000; Rubio-Gozalbo et al., 2004). Specifically, patients with CACT deficiency display elevated plasma acyl-carnitines (AC), hypoketotic hypoglycemia, hyperammonemia, ventricular arrhythmia, seizures, and progressive muscle weakness.

While the clinical manifestations of CACT deficiency have been well documented, mechanisms that control *CACT* gene expression remain poorly understood. Our current understanding is that metabolic adaptability of skeletal muscle is achieved through transcriptional networks that coordinate gene expression with fuel availability. Thus, transcription factors including PPARα, PPARδ, and FOXO along with coregulators such as PGC-1α regulate skeletal muscle fatty acid metabolism (Holloway et al., 2009). Another family of modulators with emergent influence on metabolic transcriptional responses are the Steroid Receptor Coactivators (SRCs) (York and O'Malley, 2010). The SRCs perform pleiotropic functions in diverse metabolic processes such as glycogenolysis, gluconeogenesis, dietary fat absorption and lipid storage (York and O'Malley, 2010). In particular, loss of SRC-3 has been shown to protect against obesity and improves peripheral insulin sensitivity, partly through crosstalk with PGC-1α (Coste et al., 2008). Recent evidence also suggests that functional impairment of the post-translational modification code of SRC-3 is sufficient to impair whole body metabolism (York et al., 2010). Although a number of studies have identified clear metabolic roles for SRC-3, our understanding of the physiological mechanisms that control SRC-3 expression are currently incomplete. We do know that hepatic *SRC-3* gene expression is elevated upon fasting (Louet et al., 2010), while in skeletal muscle, fasting appears to impose a modest decrease in protein expression (Coste et al., 2008). While these findings provide some elementary insight into possible regulatory inputs for SRC-3 expression, they fail to define how these physiological conditions impact SRC-3 activity.

To better understand how SRC-3 expression and activity influence intermediary metabolism, we performed a comprehensive metabolomics-based analysis to investigate how loss of this central coactivator globally impacts metabolism in a tissue- and pathway-specific manner. These data revealed a metabolic signature that was unique to SRC-3 relative to SRC-1 or 2, and specific to skeletal muscle. Expanding on these findings, we provide evidence that SRC-3 is necessary for proper transport and metabolism of long chain fatty acids, likely

through the regulation of *CACT* gene expression. Mice lacking SRC-3 display a marked deficiency in *CACT* expression, which is accompanied by elevated long chain AC, hypoketonemia, hypoglycemia, cardiac abnormality, hyperammonemia, abnormal electrical discharge in the brain, and severe muscle weakness, all of which are phenotypes associated with CACT deficiency in humans. Our studies therefore introduce another biological player in the regulation of skeletal muscle fatty acid oxidation that may contribute to unexplained disorders of lipid homeostasis.

Results

Ablation of SRC-3 results in accumulation of long chain fatty acids

To better understand the unique tissue- and pathway-specific metabolic functions of the SRC family of coactivators, we performed a comprehensive metabolomics screen using mass spectrometry on the core metabolic tissues (plasma, liver, and skeletal muscle) from male SRC-1, SRC-2 and SRC-3 wild-type and knockout littermate mice fed *ad libitum* or following a 24 hr fast. A quantitative comparison of metabolites (amino acids, organic acids and acyl-carnitines (AC)) revealed both tissue- and pathway-specific phenotypes for the SRCs (Fig. 1a). Interestingly, in SRC-$3^{+/+}$ mice, a large increase is observed in long chain AC in the skeletal muscle in the fasted compared to the *ad libitum* fed state, consistent with increased fatty acid availability and reliance on β-oxidation in this condition. In contrast, long chain ACs are elevated in both the fed and fasted states in SRC-$3^{-/-}$ mice, such that these metabolites accumulate in the fed state within the muscle of these animals (Figs. 1b and 1c). It is important to note that under fasting conditions, both SRC-$3^{+/+}$ and SRC-$3^{-/-}$ mice show similar high levels of muscle acyl-carnitines, as might be anticipated under conditions where lipolysis is active. Normally, this condition results in a maximal rate of utilization of fatty acid substrates by the muscle, which is observed in SRC-$3^{+/+}$ mice as a sharp drop in acyl-carntine levels in the fed compared to the fasted state. Conversely, no such decrease is evident in the muscles of SRC-$3^{-/-}$ mice (Fig. 1c). Moreover, the disruption of long chain fatty acid metabolism observed in the absence of SRC-3 is mirrored for the short and medium chain AC, which also show a lack of response to feeding in SRC-$3^{-/-}$ mice (Fig. S1a). Importantly, these effects were not observed upon genetic deletion of either SRC-1 or SRC-2 (Fig. S1b), suggesting a unique role for SRC-3 in skeletal muscle.

Utilization of long and very long chain fatty acids relies on a facilitated transport system, comprised of the mitochondrial proteins CPT1, CACT and CPT2. Targeted qPCR screening of muscle tissues taken from the same mice as used for metabolomics analysis identified a significant reduction in *CACT* gene expression in SRC-$3^{-/-}$ compared to SRC-$3^{+/+}$ mice (Fig. 1d). Interestingly, loss of SRC-3 conferred no alterations in 12 other genes that are essential for fatty acid entry, transport, β-oxidation, and ketogenesis (Table 1), suggesting *CACT* is a specific target of SRC-3. To determine if other p160 family members also regulate *CACT* gene expression, we analyzed its expression in muscles of SRC-1 and SRC-2 null mice. Consistent with the metabolomics data, loss of SRC-1 or SRC-2 did not significantly influence *CACT* gene expression, suggesting SRC-3-specific regulation of *CACT* in the muscle (Fig. S1c). To demonstrate that SRC-3 ablation leads to a substantial reduction of CACT protein in the muscle in both the fed and fasted states, we performed Western blot analysis (Fig. 1e and Fig. S1d) and immunohistochemistry (Fig. 1f).

Loss of SRC-3 resembles the clinical hallmarks of human CACT deficiency

Mutations or insufficiency of the *CACT* gene result in clinical symptoms of elevated long (and very long) chain fatty acids, hypoketonemia, hypoglycemia, and muscle weakness. In response to sustained exercise, when the demand for muscular fatty acid metabolism is high, SRC-3 null animals showed a marked reduction in plasma ketone concentration (Fig. 2a),

suggesting an impairment of fatty acid oxidation in the skeletal muscle. Hypoglycemia can occur as a consequence of the inability to oxidize long chain fatty acids as the demand for glucose metabolism increases. Consistent with this finding, SRC-3 null animals are hypoglycemic under both refed and fasted conditions (Fig. 2b). We performed glucose and insulin tolerance tests in SRC-$3^{+/+}$ and SRC-$3^{-/-}$ mice, but observed no clear differences in glucose homeostasis (Fig. S2a). However, hyperinsulinemic-euglycemic clamp studies revealed that ablation of SRC-3 renders animals more insulin sensitive, as indicated by the increased rate of glucose infusion required to maintain euglycemia during the hyperinsulinemic clamp, and increased whole-animal glucose disposal (Fig. 2c and Fig. S2b). Additionally, measurement of insulin levels during the glucose tolerance test showed a reduction of insulin in SRC-$3^{-/-}$ mice, further supporting an improvement in insulin sensitivity (Fig. S2a). Infusion of radiolabeled glucose in conscious SRC-$3^{+/+}$ and SRC-$3^{-/-}$ mice identified muscle (gastroc and soleus) as the primary driver of glucose uptake in the absence of SRC-3 (Fig. 2c). SRC-$3^{-/-}$ mice also exhibited a marked depletion of hepatic and muscle glycogen stores and an accumulation of neutral lipid (Fig.S2c and Fig. S2d), likely resulting from an inability to metabolize long chain fatty acids and preferential catabolism rather than storage of glucose in the SRC-$3^{-/-}$ mice. Gene expression analysis of muscle from SRC-$3^{+/+}$ and SRC-$3^{-/-}$ mice reveals a clear increase in hexokinases I and II in the absence of SRC-3, supporting the compensatory increase in glucose utilization in muscle (Fig. 2d).

Deficiency of CACT enzymatic function in humans impairs efficient β-oxidation of long (and very long) chain fatty acids, creating a reliance on glucose metabolism and severely diminishing the capacity of muscle for prolonged exercise. To determine if a similar phenotype develops in mice lacking SRC-3, SRC-$3^{+/+}$ and SRC-$3^{-/-}$ mice were run to exhaustion on a treadmill using a program that will promote fatty acid metabolism. Loss of SRC-3 dramatically reduces exercise capability (Fig. 2e). Our prior studies have reported that SRC-$3^{-/-}$ mice have a reduction in total body mass (Xu et al., 2000; Xu and O'Malley, 2002). To eliminate the possibility that the observed reduction in run time of SRC-$3^{-/-}$ mice was simply due to a decrease in lean muscle mass, we performed DEXA (dual-energy X-ray absorptiometry) analysis of SRC-$3^{+/+}$ and SRC-$3^{-/-}$ mice (Fig. S2e). Run times from Figure 2e were normalized for lean muscle mass and revealed a similar reduction for SRC-$3^{-/-}$ mice (Fig. S2f), suggesting that the exercise deficiency arises from dysfunction of the muscle, rather than a decrease in muscle mass. Cytochemical analysis of muscles from SRC-$3^{+/+}$ and SRC-$3^{-/-}$ mice shows a trend towards an increase in fast twitch fiber type in the latter group (Fig. S2g), which is further supported by qPCR analysis of gene markers for different fiber types (type I: *Myh1*; type IIa: *Myh2*; and type IIb: *Myh4*) (Fig. S2h). We propose that the impairment of SRC-3 null animals to efficiently metabolize long chain fatty acids creates a demand for glucose by the skeletal muscle (as observed by hyperinsulinemic-euglycemic clamp), which ultimately drives a transition from a slow (fatty acid utilizing) to a fast (glucose utilizing) twitch fiber type. To exclude the possibility that altered lipid delivery to the skeletal muscle contributes to these phenotypes, we analyzed plasma free fatty acids, triglycerides, as well as skeletal muscle triglycerides from SRC-$3^{+/+}$ and SRC-$3^{-/-}$ mice (Fig. S2i). These data show no significant differences in plasma free fatty acids or triglycerides, but reveal an accumulation of muscle triglycerides that is consistent with both our metabolomic and cytochemical analyses (Figs. 1b and c and Fig. S2d).

To further investigate the impact of SRC-3 loss on metabolic adaptability, we performed indirect calorimetry on SRC-$3^{+/+}$ and SRC-$3^{-/-}$ mice under the same exercise conditions utilized in Figure 2e. Analysis of the respiratory quotient compiled into quartiles of run time show an impaired ability of SRC-$3^{-/-}$ mice to transition from carbohydrate to fatty acid utilization as compared to SRC-$3^{+/+}$ mice (Fig. 2f). Additionally, we tested home cage activity of SRC-$3^{+/+}$ and SRC-$3^{-/-}$ mice and found no differences in basal activity of

SRC-$3^{+/+}$ and SRC-$3^{-/-}$ mice (Fig. S2j), thus eliminating the possibility that the decreased run time in SRC-$3^{-/-}$ mice was influenced by a reduction in basal activity. Collectively, these data showed that loss of SRC-3 resembles the primary symptoms of CACT deficiency observed in humans.

SRC-$3^{-/-}$ mice display secondary metabolic defects resulting from CACT deficiency

The primary metabolic effects of *CACT* gene deficiency related to impairment of fatty acid oxidation give rise to a number of secondary phenotypes, including hyperammonemia, cardiac arrhythmia and seizures. While no consensus exists on the etiology of the resulting hyperammonemia, two leading hypotheses are increased proteolysis to provide the substrates for *de novo* carnitine biosynthesis and impaired urea cycle function (Roschinger et al., 2000). Metabolomics analysis of plasma from SRC-$3^{+/+}$ and SRC-$3^{-/-}$ mice shows that SRC-3 knockout causes an increase in levels of 15 amino acids, with these increases attaining statistical significance for 9 of the analytes (Fig. 3a and Fig. S3a). This global increase in circulating amino acids is likely due to increased protein catabolism. The free ammonia generated from protein catabolism is metabolized in the liver via the urea cycle. Initiation of the urea cycle requires N-acetylglutamate, which is synthesized from acetyl-CoA and glutatmate. Metabolomics analyses of the livers of SRC-$3^{+/+}$ and SRC-$3^{-/-}$ mice revealed a significant decrease in acetyl-carnitine (representative of acetyl-CoA) along with a concomitant increase in glutamate (Fig. 3b). These findings suggest that catabolism of amino acids is another compensatory mechanism for overcoming the deficit in mitochondrial fatty acid oxidation and hypoglycemia elicited by SRC-3 knockout, resulting in a high rate of transamination of amino acids to yield glutamate (thus the rise in this analyte), and a high rate of acetyl-CoA utilization to initiate the urea cycle (thus the fall in this analyte). This concept is supported by clear elevation in the urea cycle intermediates ornithine, citrulline, and arginine in livers of SRC-$3^{-/-}$ mice (Fig. 3b). Moreover, qPCR analysis of the key enzymes of the urea cycle shows a marked elevation in the livers of SRC-$3^{-/-}$ mice (Fig. 3c), consistent with increased levels of urea in the urine of SRC-$3^{-/-}$ mice (Fig. 3d). Collectively, the apparent increase in flux through amino acid catabolic pathways in SRC-$3^{-/-}$ mice elicits an attempt to compensate by an increase in urea cycle activity that is ultimately overwhelmed by high rates of transamination and ammonia production, resulting in hyperammonemia.

Abnormal systems metabolism affects fuel substrate availability to other metabolic organs. Two of these main organs, the brain and heart, are inherently sensitive to changes in fuel levels (Cunnane et al., 2010; Taegtmeyer et al., 2005). Echocardiogram (ECG) analysis of resting SRC-$3^{+/+}$ and SRC-$3^{-/-}$ mice exposed a variety of cardiac abnormalities elicited by loss of SRC-3 (Fig. 3e). Most notably, SRC-3 ablation leads to decreased heart rate and overall disruption of the normal ECG profile (Fig. 3e and Figs. S3b and S3c). Furthermore, electroencephalography (EEG) analysis of SRC-$3^{+/+}$ and SRC-$3^{-/-}$ mice revealed enhanced spontaneous discharge activity in the absence of SRC-3, which suggests a higher susceptibility to seizure (Fig. S3d).

Symptoms arising from impaired long chain fatty acid metabolism in SRC-$3^{-/-}$ mice are rescued by dietary intervention with short chain fatty acids

Consistent with other long chain fatty acid disorders, the most widely accepted therapy for treating CACT deficiency is dietary supplementation of short and medium chain fatty acids, coupled with restricted intake of long (and very long) chain fatty acids (Laforet and Vianey-Saban, 2010; Wilcken, 2010). SRC-$3^{+/+}$ and SRC-$3^{-/-}$ mice were placed on diets enriched in either short/medium chain fatty acid (SCD) or long/very long chain fatty acids (LCD) for 10 weeks. Body weight measurements made over the 10-week feeding period shows that SRC-$3^{+/+}$ and SRC-$3^{-/-}$ mice gain weight normally and independent of diet (Fig. S4a).

SRC-$3^{+/+}$ and SRC-$3^{-/-}$ mice placed on SCD or LCD were subjected to treadmill exercise under conditions used in Figure 2e. These data demonstrate that SRC-$3^{-/-}$ mice respond to SCD with improved run times as compared to SRC-$3^{+/+}$ littermates, while on chow or LCD, SRC-$3^{-/-}$ mice remain significantly impaired (Fig. 4a, left panel). It is important to note that consistent with published data (Koonen et al., 2010), mice fed a SCD show a marginal reduction in absolute run time resulting primarily from the decreased energetic potential of short chain fatty acids (Fig. 4a, right panel). Indirect calorimetry of SRC-$3^{+/+}$ and SRC-$3^{-/-}$ mice on SCD show no difference between groups in RQ (Fig. 4b), as compared to chow feeding, where the separation between groups and metabolic inflexibility is clearly apparent (Fig 2f). Importantly, the SCD diet also rescued the hypoketonemia observed in SRC$3^{-/-}$ mice on either normal chow or LCD diets. LCD supplementation actually exacerbated this condition (Fig. 4c). Similarly, dietary intervention with SCD in SRC-$3^{-/-}$ mice was sufficient to restore normoglycemia, while feeding LCD resulted in a more severe hypoglycemic condition (Fig. 4d). Moreover, metabolomics data obtained from SRC-$3^{-/-}$ mice placed on SCD showed normalization of long and very long chain AC profiles (Fig. 4e) and overall improvement of amino acid levels when compared to SRC-$3^{+/+}$ mice (Fig. 4f), while feeding a LCD resulted in AC and amino acid profiles that closely resembled *SRC-3*$^{-/-}$ mice on normal chow (Figs. S4b and S4c). Taken together, these findings suggest that dietary supplementation of short/medium chain fatty acids is sufficient to improve the majority of the clinical symptoms arising from a deficit in *CACT* gene expression in *SRC-3*$^{-/-}$ mice.

SRC-3 directly regulates CACT expression in a cell-autonomous manner

Despite the central importance of CACT in long chain fatty acid metabolism, little is known regarding the regulation of *CACT* gene expression. Our data establish that *in vivo* ablation of SRC-3 leads to a significant reduction of *CACT* expression in muscle. To investigate the mechanistic underpinnings of SRC-3 regulation of *CACT* gene expression, we performed siRNA knockdown of SRC-3 in the mouse myoblast cell line, C2C12 (Fig. 5a). Knockdown of SRC-3 in C2C12 cells resulted in a significant reduction of *CACT* gene expression (Fig. 5b, i and ii), supporting a cell-autonomous role for SRC-3.

To directly test the effect of SRC-3 on *CACT* expression, we performed luciferase reporter gene assays using the *CACT* proximal promoter (−955 to +133). These data demonstrate that overexpression of SRC-3 robustly activates transcription of the *CACT* promoter (Fig. 5c). To identify the transcription factor(s) (TFs) that SRC-3 cooperates with to regulate *CACT* gene expression, we performed an *in silico* analysis (www.genomatix.de) of the *CACT* promoter for TF binding sites and cross-referenced that information with ChIP-Seq data from the ENCODE database (genome.ucsc.edu/ENCODE/). Combined, these analyses identified four putative candidate TFs: HNF1α, HNF4α, RXR/PPARα and RXR/PPARδ. SRC-3 coactivated transcription of the *CACT* promoter with each of these TFs (data not shown), suggesting that *in vivo*, SRC-3 cooperates with multiple TFs to maintain *CACT* gene expression (Iordanidou et al., 2005; Lim et al., 2004; Soutoglou et al., 2000). To determine if SRC-3 occupies the *CACT* promoter we performed chromatin immunoprecipitation (ChIP) assays in C2C12 cells using control antibody (IgG) or antibody specific for SRC-3 (Fig. 5d). These data clearly demonstrate occupancy of SRC-3 at the *CACT* promoter, but not at an unconserved adjacent region (Fig. 5c). To confirm these data *in vivo*, we performed ChIP assays using skeletal muscles isolated from SRC-$3^{+/+}$ and SRC-$3^{-/-}$ mice (Fig. 5e). Taken together, these results indicate that SRC-3 occupies the *CACT* promoter and serves a potent coactivator of *CACT* gene expression in muscle.

Discussion

In the present study, we applied metabolomics tools to gain a more in depth understanding of the metabolic functions of the p160 family of Steroid Receptor Coactivators (SRCs). These data directed us to a tissue (skeletal muscle) and pathway (long chain fatty acid catabolism) in which SRC-3 is having key metabolic effects. Mechanistically, SRC-3 performs this function by serving as a key transcriptional coactivator of *CACT*, which is necessary for mitochondrial long chain fatty acid metabolism. We have shown that loss of SRC-3 leads to a marked deficit of *CACT* gene expression, which likely contributes to impaired mitochondrial entry of long and very long chain fatty acids in the muscle, resulting in their accumulation. Consequently, loss of SRC-3 results in a compilation of phenotypes that mimic the clinical symptoms of CACT deficiency in humans. The clinical hallmarks of *CACT* deficiency arise from a combination of energy depletion and metabolic toxicity. Mice lacking SRC-3 are unable to metabolize long chain fatty acids in muscle, which ultimately accumulate in the muscle and plasma and cannot be used to generate ATP. The resulting muscle ATP deficit creates an increased demand for glucose metabolism, which coupled with the impairment of mitochondrial β-oxidation, leads to hypoketotic hypoglycemia. As a result, SRC-3$^{-/-}$ mice display increased insulin sensitivity as determined by hyperinsulinemic/euglycemic clamp, which has been reported in other cases of impaired fatty acid oxidation (Koves et al., 2008). Unique to CACT deficiency, we also observe compensatory protein catabolism that leads to increases in levels of multiple amino acids, and an induction in urea cycle activity, which is ultimately insufficient to prevent hyperammonemia from increased amino acid catabolism. SRC-3 deficiency also impairs skeletal muscle performance, and secondarily, cardiac and neurological function. While it is difficult to pinpoint the exact etiology of these phenotypes due to the broad metabolic impact on multiple tissue systems (i.e. skeletal muscle versus cardiac muscle), the effects of this syndrome that arise from loss of SRC-3 situate this important coactivator at an essential interface between fuel demand and utilization.

Our findings suggest that SRC-3 may coordinately govern diverse metabolic signaling inputs by bridging the transcriptional gaps between lipid and glucose metabolism. Work from our laboratory and others have established that disruption of SRC-3 function or expression is sufficient to confer wholesale changes in gross metabolic functions, although a metabolomics approach such as that taken here has not been reported previously. Our previously published findings demonstrate that loss of SRC-3 provides protection against high fat diet-induced obesity, partially due to an increase in PGC-1 activity (Coste et al., 2008). While the prior study reported on the role of SRC-3 in energy expenditure (reported as VO_2), fat oxidative capacity, and endurance capability, a direct comparison of those findings with the current study is not possible because of differences in data representation, diet (high fat versus normal chow), and genetic background. With regard to data representation, Coste et al reports an increase in VO_2 in the SRC-3$^{-/-}$ as evidence of improved energy expenditure, whereas we represent these data in terms of respiratory quotient (RQ = VCO_2/VO_2). It is important to note that analysis of the VO_2 parameter from the current study is directly in line with the findings of Coste et al (data not shown). In addition to the metabolic consequences arising from ablation of SRC-3, we have reported that alteration of its post-translational modification code confers onset of the metabolic syndrome (Coste et al., 2008; York et al., 2010). Collectively, these disparate phenotypes highlight the broad metabolic contributions of SRC-3 and implicate this coactivator as a key player in maintenance of the energy landscape.

At first glance, it is tempting to view the SRCs as simple generic amplifiers of transcription, but repeatedly it has been shown that their regulatory potency lies in the physiologic specificity of their target genes (Chopra et al., 2011; Chopra et al., 2008; Duteil et al., 2010).

Our findings here lend further credence to this model by demonstrating that SRC-3 does not regulate the breadth of fatty oxidation genes, but rather specifically controls the gatekeeper for long chain fatty acid metabolism in muscle, CACT. This scenario is mirrored by our recent work showing that loss of SRC-2 mimics the clinical hallmarks of human glycogen storage disease (type 1a) due to specific impairment of *G6Pase* expression, which is necessary for hepatic glucose production in response to fasting (Chopra et al., 2008). Collectively, these findings compel us to consider the SRCs as putative polygenic inputs to previously defined metabolic syndromes with assumed monogenic origins.

Consistent with the hypothesis that SRC-3 is a major regulator of CACT expression, one might predict that dysfunctional mutations in SRC-3 could account for patients that present with symptoms of CACT deficiency, but harbor no pathogenic mutations in the *CACT* gene. To investigate this possibility, we identified 24 clinical patients who exhibited CACT deficient-like symptoms, but failed to show any deleterious mutations in *CACT*. In these 24 patients, we sequenced the entire coding exons and at least 50 base pairs of their flanking intron regions of the *SRC-3* gene (*NCOA3*). While definitive deleterious mutations were not identified (Supplemental Table 1), several patients harbored heterozygous missense variants of unknown clinical significance, and a patient had an intronic variant that possibly altered splicing. In addition, 44% of patients carried heterozygous deletion of 1 or 3 glutamine residues in the polymorphic poly-glutamine tract near the C-terminus of SRC-3. While full investigation into the mechanistic impact that these mutations confer to SRC-3 expression, stability or function is beyond the scope of the current study, the identification of these genetic variations in this finite patient population is consistent with a role for SRC-3 in unexplained cases of fatty acid oxidation disorders.

In addition to these findings, the role of SRC-3 as a platform coactivator is further supported by the heterogeneity of transcription factors (TFs) predicted to regulate *CACT* gene expression (i.e. HNF1α, HNF4α, RXR/PPARα and RXR/PPARδ) (Gutgesell et al., 2009; Tachibana et al., 2009), Importantly, expression levels of these factors are not influenced by loss of SRC-3 (data not shown). Moreover, our data clearly supports the occupancy of the CACT promoter by SRC-3, suggesting that it plays a direct role in regulation of CACT expression. While it is likely that these TFs respond to multiple signaling inputs to maintain *CACT* gene expression, the efficacy of these factors hinges on the limited availability of SRC-3 to optimally drive transcription. Therefore, in the case of monogenic diseases such as CACT deficiency, while loss of a central coactivator like SRC-3 may not yield a *bona fide* phenocopy of the human disease, ablation of SRC-3 is sufficient to mimic the complete symptoms arising from genetic inactivation of CACT. These findings are of clinical interest because they underscore the SRCs as potential contributors to the etiology of previously defined monogenic diseases.

Methods

Animals

All animal experiments were performed in accordance with the Animal Care Research Committee at Baylor College of Medicine. The generation of the SRC-$1^{-/-}$, SRC-$2^{-/-}$, and SRC-$3^{-/-}$ mice has been described previously (Gehin et al., 2002; Qi et al., 1999; Xu et al., 2000). Only male, age-matched littermate (10–16 weeks old) mice were used. Animals were maintained in a temperature controlled (23°C) facility with a 12-hr light/dark cycle. Mice on normal chow were fed 2920X Teklad Global rodent *ad libitum* with free access to food and water, or fasted for 24 hrs with access to water only as indicated. Separate cohorts of SRC-$3^{+/+}$ and SRC-$3^{-/-}$ littermate male mice were maintained on either short chain fatty acid enriched diet (SCD: Harlan Teklad TD.09849 (1FO : 1 Lard)) or a long chain fatty acid enriched diet (LCD: Harlan Teklad TD.09848 (1CCO : 1HCCO)) for 10 weeks.

Metabolomic profiling

Metabolomics analyses have been described in detail elsewhere (An et al., 2004; Haqq et al., 2005; Newgard et al., 2009). Briefly, amino acids, acyl-carnitines and organic acids were measured using stable isotope dilution techniques. Amino acids and acyl-carnitine species were measured using flow injection tandem mass spectrometry and sample preparation methods described previously (An et al., 2004; Haqq et al., 2005). Data was acquired using a Micromass Quattro micro TM system equipped with a model 2777 autosampler, a model 1525 μ HPLC solvent delivery system, and a data system controlled by MassLynx 4.0 operating system (Waters, Milford, MA). Organic acids were quantified using a previously described method using Trace GC Ultra coupled to a Trace DSQ MS operating under Excalibur 1.4 (Thermo Fisher Scientific, Austin, TX). All MS analyses employed stable-isotope-dilution. The standard allows for identification of each analytes peak, and provides the reference for quantifying their levels. Quantification was facilitated by addition of mixtures of known quantities of stable-isotope internal standards to samples exactly as described (An et al., 2004; Haqq et al., 2005). In addition to mass, analytes are identified on the basis of the particular MS/MS transitions that we monitor for each class of metabolite.

qPCR Assays

Total mRNA was isolated from muscle or liver using the RNeasy Kit (Qiagen). Reverse transcription was carried out using Superscript III (Invitrogen) per the manufacturer's instructions. For gene expression analysis, qPCR was performed using the Taqman system with sequence-specific primers and the Universal Probe Library (Roche). For all analyses, 18S rRNA was used as an internal control. Sequences of qPCR primers are available upon request.

Hyperinsulinemic/Euglycemic Clamp

Glucose clamp studies and tissue specific glucose uptake were performed as previously described (Saha et al., 2004). Briefly, mice were anesthetized and cannulated followed by a 3–4 day recovery. Mice were fasted overnight then administered a primed infusion (10 mCi) followed by a constant intravenous infusion (0.1 mCi/min) of [3-^{3}H]-glucose (Perkin Elmer Life Sciences). Basal glucose production was measured by tail vein bleed 60 mins after glucose infusion. Mice were then primed with regular insulin (40 millunits/kg BW) followed by a 2-hr insulin infusion (3 millunitsw/kg/min) while simultaneously infusing 10% glucose at a rate adjusted to maintain blood glucose between 100–140 mg/dl. Blood glucose concentrations were determined every 10 mins by a handheld glucometer (Lifescan). Following a 120-min period, blood was collected to determine hepatic glucose production and glucose disposal rates.

Treadmill Endurance Tests

SRC-3$^{+/+}$ and SRC-3$^{-/-}$ mice were acclimated to treadmill running (5 meters/min for 3 mins) prior to testing. For endurance testing, acclimated mice were run on a treadmill at a 10° incline at a constant speed of 15 meters/min until exhaustion.

Statistical Analyses

All results are shown as the mean ± standard error mean (s.e.m.). Standard statistical comparison of different groups with Gaussian distribution was carried out using two-tailed unpaired Student's *t* test. For analysis of the *in vivo* ChIP data, the Mann-Whitney U test was used due to a non-Gaussian distribution and limited sample size. Statistical analysis of area under the curve (AUC) time-course measurements of glucose and insulin tolerance tests was performed using a two-way ANOVA (experimental variables = time and genotype). For all statistical analyses, differences of $P \leq 0.05$ were considered statistically significant. For

all mice studies, the experimental number used is indicated in each figure legend. For all other studies, experiments were repeated at least three times.

Supplementary Material

Refer to Web version on PubMed Central for supplementary material.

Acknowledgments

We especially thank Adam Dean and Pauline Grennan for technical assistance. Special thanks to Rainer Lanz for bioinformatic analysis of the *CACT* promoter. Jørn V. Sagen is funded by the Norwegian Cancer Society, University of Bergen, Det regionale samarbeidsorganet (Helse Vest RHF and University of Bergen), and the Norwegian Society of Endocrinology. Thanks to Lawrence Chan and Pradip Saha at the NIDDK sponsored MMC Core at BCM under DERC (P30 DK079638) for assistance with the clamp studies. Also, we kindly thank Robert Ringseis for *CACT* luciferase reporter constructs. This work was supported by R01 DK058242 & R01 CA112403 to J. Xu, NURSA/NIDDK U19 DK62434-08 to B.W. O'Malley and C.B. Newgard, NIDDK PO1 HD08818-37 to B.W. O'Malley, and R01HD8188-38S1 to B. York and B.W O'Malley.

References

An J, Muoio DM, Shiota M, Fujimoto Y, Cline GW, Shulman GI, Koves TR, Stevens R, Millington D, Newgard CB. Hepatic expression of malonyl-CoA decarboxylase reverses muscle, liver and whole-animal insulin resistance. Nat Med. 2004; 10:268–274. [PubMed: 14770177]

Chang BH, Liao W, Li L, Nakamuta M, Mack D, Chan L. Liver-specific inactivation of the abetalipoproteinemia gene completely abrogates very low density lipoprotein/low density lipoprotein production in a viable conditional knockout mouse. J Biol Chem. 1999; 274:6051–6055. [PubMed: 10037685]

Chen X, Liu Z, Xu J. The cooperative function of nuclear receptor coactivator 1 (NCOA1) and NCOA3 in placental development and embryo survival. Mol Endocrinol. 2010; 24:1917–1934. [PubMed: 20685850]

Chopra AR, Kommagani R, Saha P, Louet JF, Salazar C, Song J, Jeong J, Finegold M, Viollet B, DeMayo F, Chan L, Moore DD, O'Malley BW. Cellular energy depletion resets whole-body energy by promoting coactivator-mediated dietary fuel absorption. Cell Metab. 2011; 13:35–43. [PubMed: 21195347]

Chopra AR, Louet JF, Saha P, An J, Demayo F, Xu J, York B, Karpen S, Finegold M, Moore D, Chan L, Newgard CB, O'Malley BW. Absence of the SRC-2 coactivator results in a glycogenopathy resembling Von Gierke's disease. Science. 2008; 322:1395–1399. [PubMed: 19039140]

Coste A, Louet JF, Lagouge M, Lerin C, Antal MC, Meziane H, Schoonjans K, Puigserver P, O'Malley BW, Auwerx J. The genetic ablation of SRC-3 protects against obesity and improves insulin sensitivity by reducing the acetylation of PGC-1{alpha}. Proc Natl Acad Sci U S A. 2008; 105:17187–17192. [PubMed: 18957541]

Cunnane S, Nugent S, Roy M, Courchesne-Loyer A, Croteau E, Tremblay S, Castellano A, Pifferi F, Bocti C, Paquet N, Begdouri H, Bentourkia M, Turcotte E, Allard M, Barberger-Gateau P, Fulop T, Rapoport SI. Brain fuel metabolism, aging, and Alzheimer's disease. Nutrition. 2010; 27:3–20. [PubMed: 21035308]

Duteil D, Chambon C, Ali F, Malivindi R, Zoll J, Kato S, Geny B, Chambon P, Metzger D. The transcriptional coregulators TIF2 and SRC-1 regulate energy homeostasis by modulating mitochondrial respiration in skeletal muscles. Cell Metab. 2010; 12:496–508. [PubMed: 21035760]

Eaton S, Bartlett K, Pourfarzam M. Mammalian mitochondrial beta-oxidation. Biochem J. 1996; 320 (Pt 2):345–357. [PubMed: 8973539]

Gehin M, Mark M, Dennefeld C, Dierich A, Gronemeyer H, Chambon P. The function of TIF2/GRIP1 in mouse reproduction is distinct from those of SRC-1 and p/CIP. Mol Cell Biol. 2002; 22:5923–5937. [PubMed: 12138202]

Gutgesell A, Wen G, Konig B, Koch A, Spielmann J, Stangl GI, Eder K, Ringseis R. Mouse carnitine-acylcarnitine translocase (CACT) is transcriptionally regulated by PPARalpha and PPARdelta in liver cells. Biochim Biophys Acta. 2009; 1790:1206–1216. [PubMed: 19577614]

Haqq AM, Lien LF, Boan J, Arlotto M, Slentz CA, Muehlbauer MJ, Rochon J, Gallup D, McMahon RL, Bain JR, Stevens R, Millington D, Butler MD, Newgard CB, Svetkey LP. The Study of the Effects of Diet on Metabolism and Nutrition (STEDMAN) weight loss project: Rationale and design. Contemp Clin Trials. 2005; 26:616–625. [PubMed: 16239128]

Holloway GP, Bonen A, Spriet LL. Regulation of skeletal muscle mitochondrial fatty acid metabolism in lean and obese individuals. Am J Clin Nutr. 2009; 89:455S–462S. [PubMed: 19056573]

Iordanidou P, Aggelidou E, Demetriades C, Hadzopoulou-Cladaras M. Distinct amino acid residues may be involved in coactivator and ligand interactions in hepatocyte nuclear factor-4alpha. J Biol Chem. 2005; 280:21810–21819. [PubMed: 15826954]

Koonen DP, Sung MM, Kao CK, Dolinsky VW, Koves TR, Ilkayeva O, Jacobs RL, Vance DE, Light PE, Muoio DM, Febbraio M, Dyck JR. Alterations in skeletal muscle fatty acid handling predisposes middle-aged mice to diet-induced insulin resistance. Diabetes. 2010; 59:1366–1375. [PubMed: 20299464]

Koves TR, Ussher JR, Noland RC, Slentz D, Mosedale M, Ilkayeva O, Bain J, Stevens R, Dyck JR, Newgard CB, Lopaschuk GD, Muoio DM. Mitochondrial overload and incomplete fatty acid oxidation contribute to skeletal muscle insulin resistance. Cell Metab. 2008; 7:45–56. [PubMed: 18177724]

Laforet P, Vianey-Saban C. Disorders of muscle lipid metabolism: diagnostic and therapeutic challenges. Neuromuscul Disord. 2010; 20:693–700. [PubMed: 20691590]

Lim HJ, Moon I, Han K. Transcriptional cofactors exhibit differential preference toward peroxisome proliferator-activated receptors alpha and delta in uterine cells. Endocrinology. 2004; 145:2886–2895. [PubMed: 15001550]

Louet JF, Chopra AR, Sagen JV, An J, York B, Tannour-Louet M, Saha PK, Stevens RD, Wenner BR, Ilkayeva OR, Bain JR, Zhou S, DeMayo F, Xu J, Newgard CB, O'Malley BW. The coactivator SRC-1 is an essential coordinator of hepatic glucose production. Cell Metab. 2010; 12:606–618. [PubMed: 21109193]

Martinez-Botas J, Anderson JB, Tessier D, Lapillonne A, Chang BH, Quast MJ, Gorenstein D, Chen KH, Chan L. Absence of perilipin results in leanness and reverses obesity in Lepr(db/db) mice. Nat Genet. 2000; 26:474–479. [PubMed: 11101849]

McGarry JD, Brown NF. The mitochondrial carnitine palmitoyltransferase system. From concept to molecular analysis. Eur J Biochem. 1997; 244:1–14. [PubMed: 9063439]

Moczulski D, Majak I, Mamczur D. An overview of beta-oxidation disorders. Postepy Hig Med Dosw (Online). 2009; 63:266–277. [PubMed: 19535822]

Newgard CB, An J, Bain JR, Muehlbauer MJ, Stevens RD, Lien LF, Haqq AM, Shah SH, Arlotto M, Slentz CA, Rochon J, Gallup D, Ilkayeva O, Wenner BR, Yancy WS Jr, Eisenson H, Musante G, Surwit RS, Millington DS, Butler MD, Svetkey LP. A branched-chain amino acid-related metabolic signature that differentiates obese and lean humans and contributes to insulin resistance. Cell Metab. 2009; 9:311–326. [PubMed: 19356713]

Qi C, Zhu Y, Pan J, Yeldandi AV, Rao MS, Maeda N, Subbarao V, Pulikuri S, Hashimoto T, Reddy JK. Mouse steroid receptor coactivator-1 is not essential for peroxisome proliferator-activated receptor alpha-regulated gene expression. Proc Natl Acad Sci U S A. 1999; 96:1585–1590. [PubMed: 9990068]

Roschinger W, Muntau AC, Duran M, Dorland L, LIJ, Wanders RJ, Roscher AA. Carnitine-acylcarnitine translocase deficiency: metabolic consequences of an impaired mitochondrial carnitine cycle. Clin Chim Acta. 2000; 298:55–68. [PubMed: 10876004]

Rubio-Gozalbo ME, Bakker JA, Waterham HR, Wanders RJ. Carnitine-acylcarnitine translocase deficiency, clinical, biochemical and genetic aspects. Mol Aspects Med. 2004; 25:521–532. [PubMed: 15363639]

Saha PK, Kojima H, Martinez-Botas J, Sunehag AL, Chan L. Metabolic adaptations in the absence of perilipin: increased beta-oxidation and decreased hepatic glucose production associated with peripheral insulin resistance but normal glucose tolerance in perilipin-null mice. J Biol Chem. 2004; 279:35150–35158. [PubMed: 15197189]

Shim DJ, Yang L, Reed JG, Noebels JL, Chiao PJ, Zheng H. Disruption of the NF-kappaB/IkappaBalpha autoinhibitory loop improves cognitive performance and promotes hyperexcitability of hippocampal neurons. Mol Neurodegener. 2011; 6:42. [PubMed: 21663635]

Soutoglou E, Papafotiou G, Katrakili N, Talianidis I. Transcriptional activation by hepatocyte nuclear factor-1 requires synergism between multiple coactivator proteins. J Biol Chem. 2000; 275:12515–12520. [PubMed: 10777539]

Tachibana K, Takeuchi K, Inada H, Yamasaki D, Ishimoto K, Tanaka T, Hamakubo T, Sakai J, Kodama T, Doi T. Regulation of the human SLC25A20 expression by peroxisome proliferator-activated receptor alpha in human hepatoblastoma cells. Biochem Biophys Res Commun. 2009; 389:501–505. [PubMed: 19748481]

Taegtmeyer H, Wilson CR, Razeghi P, Sharma S. Metabolic energetics and genetics in the heart. Ann N Y Acad Sci. 2005; 1047:208–218. [PubMed: 16093498]

Wilcken B. Fatty acid oxidation disorders: outcome and long-term prognosis. J Inherit Metab Dis. 2010; 33:501–506. [PubMed: 20049534]

Xu J, Liao L, Ning G, Yoshida-Komiya H, Deng C, O'Malley BW. The steroid receptor coactivator SRC-3 (p/CIP/RAC3/AIB1/ACTR/TRAM-1) is required for normal growth, puberty, female reproductive function, and mammary gland development. Proc Natl Acad Sci U S A. 2000; 97:6379–6384. [PubMed: 10823921]

Xu J, O'Malley BW. Molecular mechanisms and cellular biology of the steroid receptor coactivator (SRC) family in steroid receptor function. Rev Endocr Metab Disord. 2002; 3:185–192. [PubMed: 12215713]

Yang Z, McMahon CJ, Smith LR, Bersola J, Adesina AM, Breinholt JP, Kearney DL, Dreyer WJ, Denfield SW, Price JF, Grenier M, Kertesz NJ, Clunie SK, Fernbach SD, Southern JF, Berger S, Towbin JA, Bowles KR, Bowles NE. Danon disease as an underrecognized cause of hypertrophic cardiomyopathy in children. Circulation. 2005; 112:1612–1617. [PubMed: 16144992]

York B, O'Malley BW. Steroid receptor coactivator (SRC) family: masters of systems biology. J Biol Chem. 2010; 285:38743–38750. [PubMed: 20956538]

York B, Yu C, Sagen JV, Liu Z, Nikolai BC, Wu RC, Finegold M, Xu J, O'Malley BW. Reprogramming the posttranslational code of SRC-3 confers a switch in mammalian systems biology. Proc Natl Acad Sci U S A. 2010; 107:11122–11127. [PubMed: 20534466]

Highlights

- Metabolomics profiling unveils unique metabolic functions of SRCs
- SRC-3 controls long-chain fatty acid metabolism through direct regulation of *CACT*
- Ablation of *SRC-3* resembles the clinical hallmarks of CACT deficiency in humans
- Dietary intervention rescues the functional loss of SRC-3 in skeletal muscle

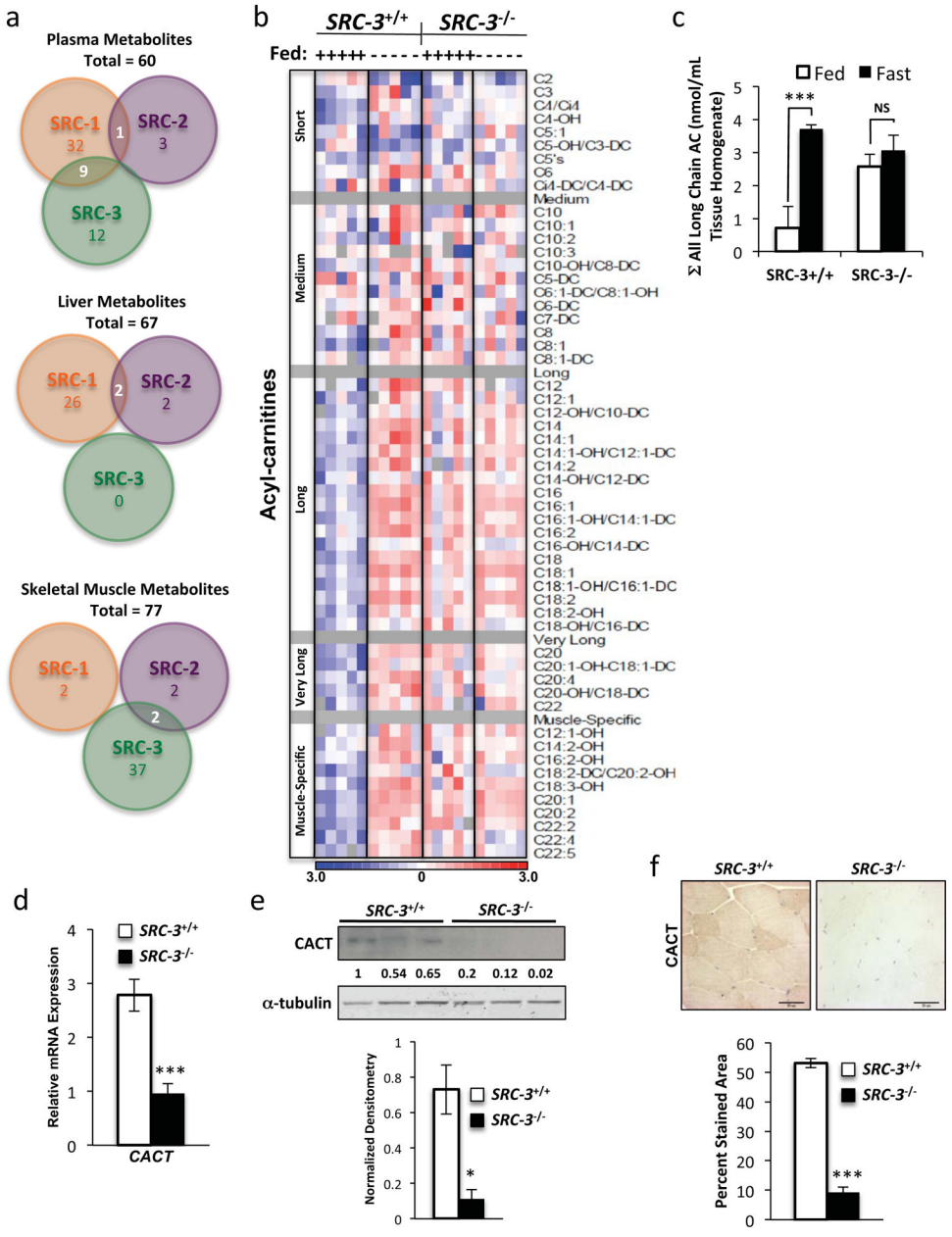

Figure 1.

Loss of SRC-3 leads to muscle-specific accumulation of long chain fatty acids.

a) Venn diagram comparison of tissue-specific mass spectrometry-based metabolomics analyses of plasma, liver, and skeletal muscle amino acids, organic acids and acyl-carnitines (AC) from SRC-1, SRC-2 and SRC-3 wild-type and knockout male mice (N = 5 each genotype). Of the total metabolites analyzed for each tissue (plasma = 60; liver = 67; muscle = 77), the numbers of metabolites that are statistically changed (either increased or decreased) by comparing each WT to its respective littermate knockout are indicated below the name of each coactivator (SRC-1, SRC-2, SRC-3). The number of statistically significant changes (either increased or decreased) in metabolites shared by more than one coactivator is indicated in overlapping regions of the Venn diagram.

b) Heat map representation of z-score transformed raw data representing varying chain length AC obtained from mass spectrometry of skeletal muscle extract isolated from SRC-$3^{+/+}$ (N = 5) and SRC-$3^{-/-}$ (N = 5) mice fed *ad libitum* or following a 24-hr fast as indicated. The heat map is set on a three-point gradient color scale with blue representing low z-score values and red representing high z-score values, respectively.
c) Graphical representation of raw data from Figure 1b representing the sum (Σ) of all long chain species AC from SRC-$3^{+/+}$ (N = 5) and SRC-$3^{-/-}$ (N = 5) mice fed *ad libitum* (white bars) or following a 24-hr fast (black bars) as indicated.
d) Quantitative real-time PCR analysis of *CACT* gene expression from skeletal muscle of SRC-$3^{+/+}$ (white bars, N = 5) and SRC-$3^{-/-}$ (black bars, N = 5) mice fed *ad libitum*. Expression levels were normalized to 18S rRNA.
e) Western blot analysis of CACT and α-tubulin protein expression in skeletal muscle protein extract isolated from SRC-$3^{+/+}$ (N = 3) and SRC-$3^{-/-}$ (N = 3) mice fed *ad libitum*. Protein levels at each time point were quantitated by densitometry using Image J software and normalized to α-tubulin and are indicated numerically under each lane. Data are graphed as the mean ± s.e.m.
f) Representative histology of skeletal muscle isolated from SRC-$3^{+/+}$ and SRC-$3^{-/-}$ mice fed *ad libitum*. Formalin fixed tissues sections were analyzed by immunohistochemistry for expression of either SRC-3 or CACT as indicated. Quantitation of the CACT signal was performed using Image Pro Plus® software. Data are graphed as the mean ± s.e.m. *P < 0.05, ***P < 0.001 versus WT mice.

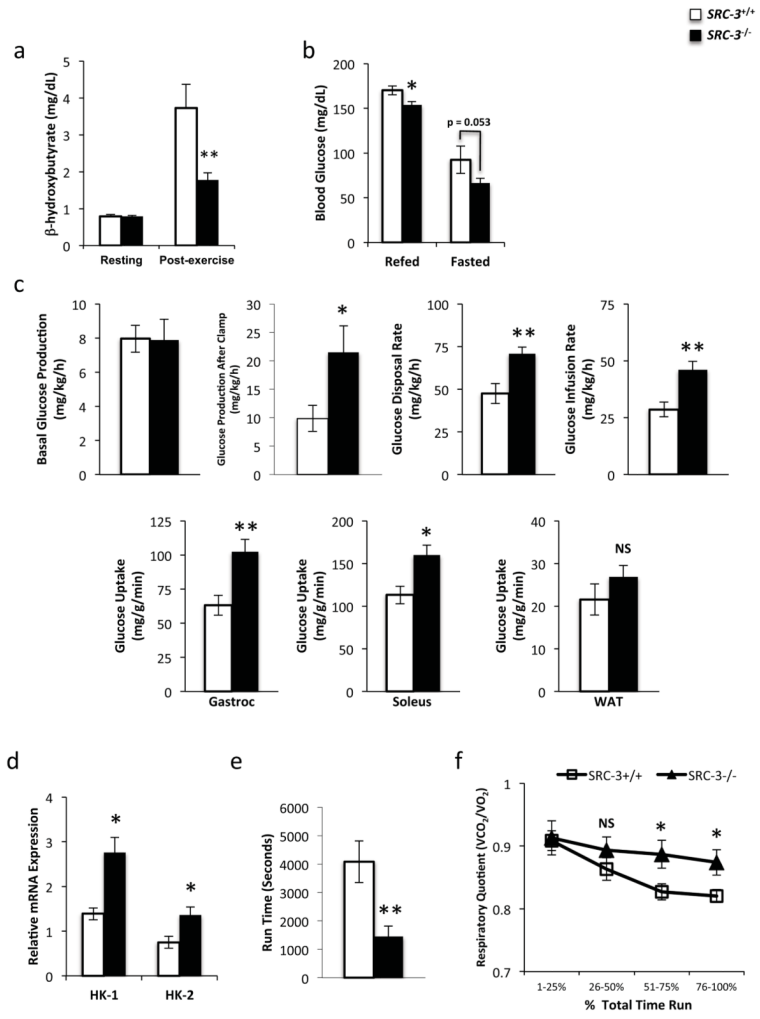

Figure 2.

Ablation of SRC-3 phenocopies the primary clinical symptoms of CACT deficiency.

a) Plasma profiling of β-hydroxybutyrate under resting (non-exercised) conditions or immediately following exhaustive exercise in SRC-$3^{+/+}$ (N = 10) and SRC-$3^{-/-}$ (N = 10) mice.

b) Measurement of blood glucose in SRC-$3^{+/+}$ (N = 5) and SRC-$3^{-/-}$ (N = 5) mice following 24-hr fasting or a 3 hr refeed after a 24-hr fast.

c) Hyperinsulinemic/euglycemic clamp analysis of basal and clamped glucose production, glucose disposal rate, glucose infusion rate, and tissue-specific (gastroc, soleus, WAT) glucose uptake measured in SRC-$3^{+/+}$ (N = 7) and SRC-$3^{-/-}$ (N = 7) mice.

d) Quantitative real-time PCR analysis of *HK-1* and *HK-2* gene expression levels in skeletal muscle of SRC-$3^{+/+}$ (white bars, N = 5) and SRC-$3^{-/-}$ (black bars, N = 5) mice fed *ad libitum*. Expression levels were normalized to 18S rRNA using the ΔΔCT method where each gene is relative to its own internal 18S rRNA control individually normalized against one SRC-$3^{+/+}$ sample.

e) Treadmill endurance exercise measurements from SRC-$3^{+/+}$ (white bars, N = 10) and SRC-$3^{-/-}$ (black bars, N = 10) mice run on a 10° incline at 15 meters/min until exhaustion.

f) Calculated respiratory quotients (VCO_2/VO_2) obtained from indirect calorimetry measurements from SRC-$3^{+/+}$ (white filled, N = 6) and SRC-$3^{-/-}$ (black filled, N = 6) mice while running on a 10° incline at 15 meters/min until exhaustion. Respiratory quotient data

are graphed as a function of total run time broken into percentage quartiles. Data are graphed as the mean ± s.e.m. *P < 0.05, **P < 0.01, NS = not statistically significant versus WT mice.

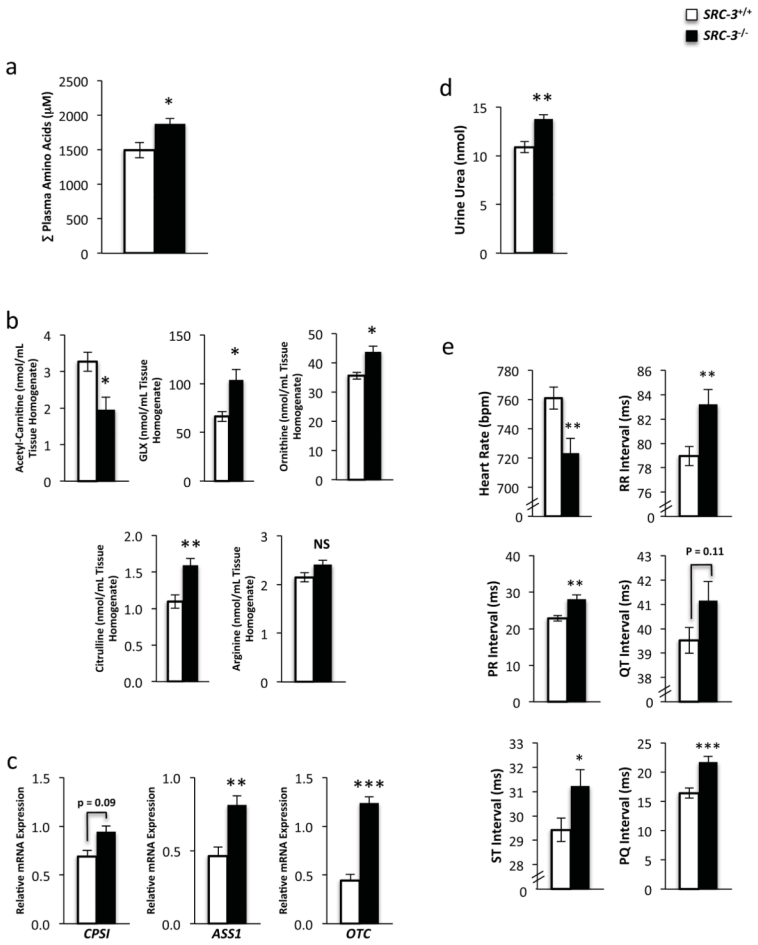

Figure 3.

SRC-$3^{-/-}$ mice display secondary metabolic defects resulting from CACT deficiency.

a) Quantitative mass spectrometric analysis of the sum of all plasma amino acids from SRC-$3^{+/+}$ (white bars, N = 5) and SRC-$3^{-/-}$ (black bars, N = 5) mice fed *ad libitum* and graphed as μM.

b) Quantitative mass spectrometric analysis of urea cycle metabolites (acetyl-carnitine, GLX (glutamate/glutamine), ornithine, citrulline, and arginine) from liver tissue extracts isolated from SRC-$3^{+/+}$ (white bars, N = 5) and SRC-$3^{-/-}$ (black bars, N = 5) mice fed *ad libitum*.

c) Quantitative real-time PCR analysis of *CPSI*, *ASS1*, and *OTC* gene expression levels in liver tissue from SRC-$3^{+/+}$ (white bars, N = 5) and SRC-$3^{-/-}$ (black bars, N = 5) mice fed *ad libitum*. All expression levels were normalized to 18S rRNA.

d) Quantitative colorimetric enzyme analysis of urine urea from SRC-$3^{+/+}$ (white bars, N = 5) and SRC-$3^{-/-}$ (black bars, N = 5) mice fed *ad libitum*.

e) Non-invasive electrocardiography analysis of resting conscious SRC-$3^{+/+}$ (white bars, N = 8) and SRC-$3^{-/-}$ (black bars, N = 8) mice fed *ad libitum*. Data presented are heart rate (beats per min), RR, PR, QT, ST and PQ intervals (milliseconds), respectively. Data are graphed as the mean ± s.e.m. *P < 0.05, **P < 0.01, ***P<0.001, NS = not statistically significant versus WT mice.

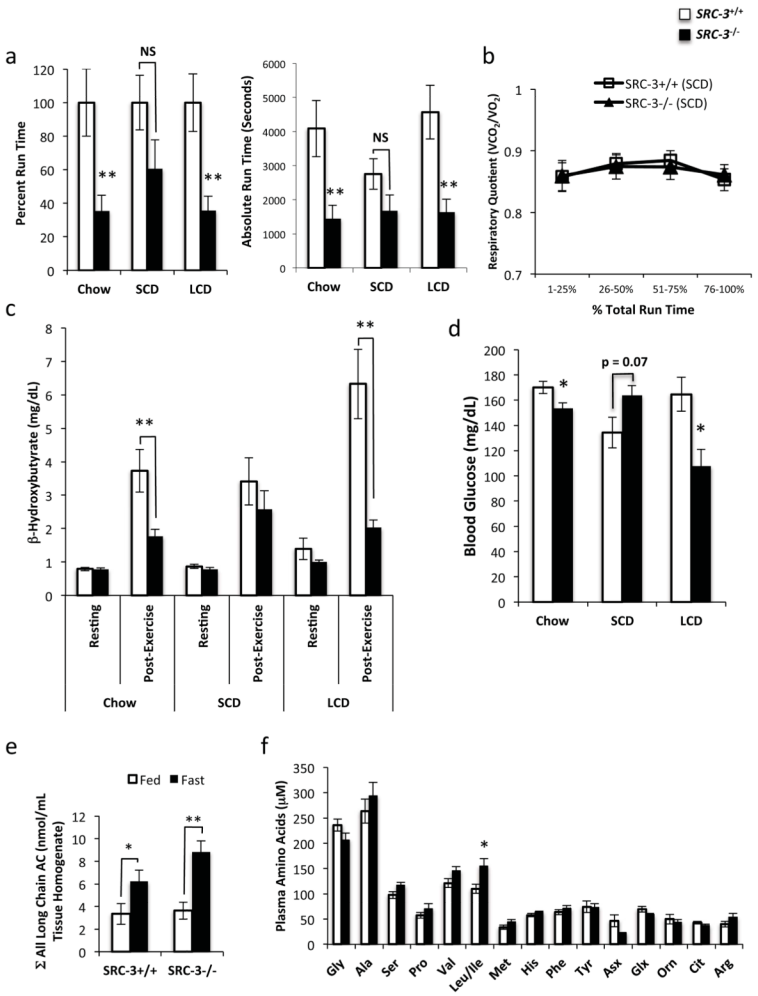

Figure 4.

Dietary treatment with short/medium chain fatty acids rescues CACT deficiency in the absence of SRC-3

a) Treadmill endurance exercise measurements from SRC-$3^{+/+}$ (white bars, N = 10) and SRC-$3^{-/-}$ (black bars, N = 10) mice run on a 10° incline at 15 meters/min until exhaustion following a 10-week regimen of normal chow (Chow), short chain fatty acid enriched diet (SCD) or long chain fatty acid enriched diet (LCD). Run time data are normalized to SRC-$3^{+/+}$ from each feeding regimen and represented as a percentage of wild-type (left panel). Raw run time data from SRC-$3^{+/+}$ and SRC-$3^{-/-}$ mice (right panel).

b) Calculated respiratory quotients (VCO_2/VO_2) obtained from indirect calorimetry measurements from SRC-$3^{+/+}$ (white filled, N = 6) and SRC-$3^{-/-}$ (black filled, N = 6) mice run on a 10° incline at 15 meters/min until exhaustion following a 10-week regimen on SCD. Respiratory quotient data are graphed as a function of total run time broken into percentage quartiles.

c) Plasma profiling of β-hydroxybutyrate under resting conditions or immediately following exhaustive exercise in SRC-$3^{+/+}$ (N = 10) and SRC-$3^{-/-}$ (N = 10) mice fed *ad libitum* on a 10-week regimen of chow, SCD or LCD.

d) Measurement of blood glucose in SRC-$3^{+/+}$ (N = 5) and SRC-$3^{-/-}$ (N = 5) mice fed *ad libitum* following a 10-week regimen of of chow, SCD or LCD.

e) Quantitative mass spectrometry analysis of AC from skeletal muscle tissue extracts isolated from SRC-$3^{+/+}$ (N = 5) and SRC-$3^{-/-}$ (N = 5) mice fed *ad libitum* (white bars) or following a 24-hr fast (black bars) after a 10-week regimen on a SCD. Data are represented as the sum (Σ) of all long chain species of AC.
f) Quantitative mass spectrometric analysis of plasma amino acids from SRC-$3^{+/+}$ (white bars, N = 5) and SRC-$3^{-/-}$ (black bars, N = 5) mice following a 10-week regimen on a SCD. Data are graphed as the mean ± s.e.m. *P < 0.05, **P < 0.01, NS = not statistically significant versus WT mice.

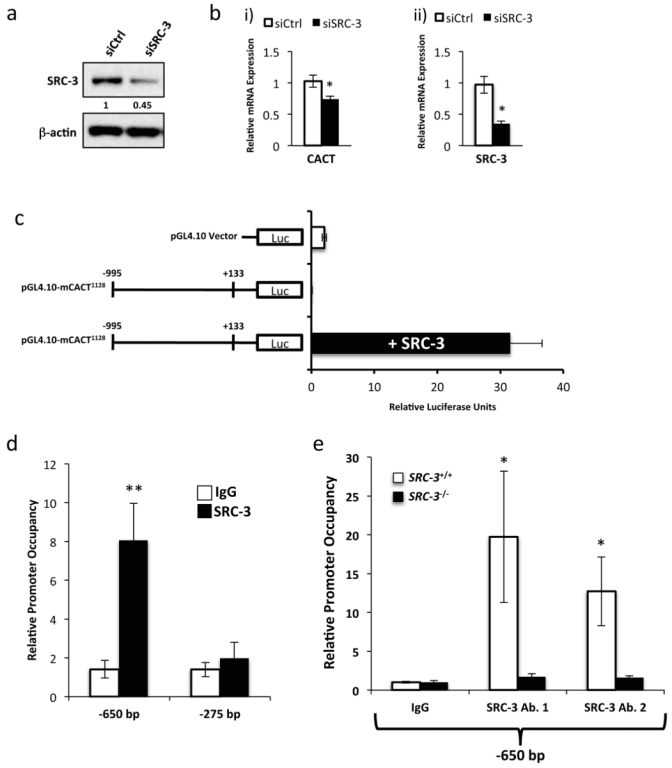

Figure 5.

SRC-3 regulation of *CACT* expression is cell-autonomous

a) Western blot analysis of SRC-3 and β-actin following siRNA knockdown of SRC-3 in C2C12 myoblasts. Protein levels for each treatment were quantitated by densitometry using Image J software and normalized to β-actin and are indicated numerically under each lane.

b) Quantitative real-time PCR analysis of *CACT* (i) and *SRC-3* (ii) gene expression in C2C12 myoblasts after transient knockdown with a non-targeting siRNA (white bars, N = 3) or siRNA against SRC-3 (black bars, N = 3). All expression levels were normalized to 18S rRNA.

c) Luciferase reporter assays from COS-1 cells transiently transfected with pGL4.10 vector alone (white bar) or pGL4.10-m*CACT*^{1128} (−995 to +133) luciferase construct in the absence or presence of SRC-3 (black bar). All luciferase data were normalized to total protein.

d) Chromatin immunoprecipitation (ChIP) of SRC-3 from C2C12 myoblasts. The amplicon is directed toward a conserved region approximately −650 bp upstream of the transcriptional start site or at an unconserved region −275 bp upstream. All data are presented as relative promoter occupancy of SRC-3 signal compared to IgG control.

e) *In vivo* ChIP of SRC-3 in skeletal muscles isolated from SRC-3$^{+/+}$ (N = 3) and SRC-3$^{-/-}$ (N = 3) mice fed *ad libitum*. The amplicon is directed toward a conserved region approximately −650 bp upstream of the transcriptional start site. All data are presented as relative promoter occupancy of SRC-3 signal compared to IgG. Data are graphed as the mean ± s.e.m. *P < 0.05, **P < 0.01 versus WT mice.

Table 1

qPCR analysis of muscle fatty acid regulatory genes.

Gene ID	Gene Name	SRC-3$^{+/+}$	SRC-3$^{-/-}$	p value
CPT1β	Carnitine Palmitoyltransferase I beta	0.703 ± 0.10	0.72 ± 0.10	0.93
CPT2	Carnitine Palmitoyltransferase 2	1.06 ± 0.09	0.91 ± 0.14	0.39
FASN	Fatty Acid Synthase	7.53 ± 5.5	6.92 ± 5.1	0.94
MCD	Malonyl-CoA Decarboxylase	1.16 ± 0.27	1.54 ± 1.17	0.31
ACC2	Acetyl-Coenzyme A Carboxylase beta	0.780 ± 0.09	0.754 ± 0.06	0.80
ACS	Acyl-CoA Synthetase	1.20 ± 0.19	1.07 ± 0.23	0.67
ACADL	Acyl-Coenzyme A Dehydrogenase, long chain	0.58 ± 0.07	0.60 ± 0.11	0.87
ACADVL	Acyl-Coenzyme A Dehydrogenase, very long chain	1.15 ± 0.17	0.87 ± 0.10	0.20
ECHS1	Enoyl Coenzyme A Hydratase, short chain, 1, mitochondrial	1.11 ± 0.14	1.03 ± 0.07	0.65
HADH	Hydroxyacyl-Coenzyme A Dehydrogenase	1.02 ± 0.12	0.88 ± 0.10	0.39
ACAA1A	Acetyl-Coenzyme A Acyltransferase 1A	1.24 ± 0.11	1.16 ± 0.10	0.59
CRAT	Carnitine Acetyltransferase	1.16 ± 0.27	1.54 ± 0.17	0.31